JOURNAL OF THERMOPHYSICS AND HEAT TRANSFER
Vol. 19, No. 4, October–December 2005

# Viscous Effects on Cooled Pitot Tubes in Hypersonic Low Reynolds Number Flows

George R. Inger*
*Iowa State University, Ames, Iowa 50011*

**The influence of low Reynolds number viscous effects on blunt-nose stagnation pressure is investigated analytically for near-continuum hypersonic ideal gas flows around cooled bodies. It is shown that normal stress within the boundary layer acts to increase stagnation pressure slightly but that the usually neglected pressure slip at the wall introduces a significant opposing effect when the wall is cooled. Closed-form relationships describing this behavior as a function of Reynolds number, wall temperature ratio, and gas type are developed and shown to agree with experiment.**

## Nomenclature

| | | |
|---|---|---|
| $a$ | = | local speed of sound |
| $C_p$ | = | pressure coefficient, $2(p - p_\infty)/\rho_\infty U_\infty^2$ |
| $C_s$, $C_G$ | = | constants, Eq. (16) |
| $D$ | = | body diameter, $2R_B$ |
| $f$ | = | boundary-layer stream function |
| $g$ | = | $[(T/T_s) - \theta w]/[1 - \theta w]$ |
| $I_{1,2}$ | = | boundary-layer integral functions, Eq. (10) |
| $j$ | = | dimensionality index, 0 for two dimensions, 1 for axisymmetric |
| $K_g$ | = | constant in heat transfer relations, Eq. (9c) |
| $Kn$ | = | Knudsen number, $\lambda/D$ |
| $K_{W_t}$, $K_{W_p}$ | = | constants, Eqs. (14) and (15) |
| $M$ | = | Mach number |
| $Pr$ | = | Prandtl number |
| $P_s$ | = | stagnation pressure |
| $p$ | = | static pressure |
| $R_B$ | = | body-nose radius (Fig. 1) |
| $Re_D$ | = | $2Re_s$ |
| $Re_s$ | = | shock layer Reynolds number, $\rho_\infty U_\infty R_B/\mu_s$ |
| $Re_{s\varepsilon}$ | = | modified Reynolds number, $Re_s/\sqrt{\varepsilon_F}$ |
| $Re_{\varepsilon D}$ | = | $Re_D/\sqrt{\varepsilon_F}$ |
| $U_\infty$ | = | freestream (flight) velocity |
| $u$, $v$ | = | velocity components along $x$ and $y$, respectively (Fig. 1) |
| $x$, $y$ | = | coordinates tangential and normal to body, respectively (Fig. 1) |
| $\alpha$ | = | thermal accommodation coefficient on body surface |
| $\beta_s$ | = | inviscid stagnation point velocity gradient |
| $\Gamma_G$ | = | parameter in Eq. (11), $\sqrt{[2(1-\varepsilon_F)](\gamma+1)/(\gamma+3)}$ |
| $\gamma$ | = | specific heat ratio of gas |
| $\varepsilon_F$ | = | limiting density ratio across a strong normal shock, $\rho_\infty/\rho_s = (\gamma-1)(\gamma+1)$ |
| $\eta$ | = | boundary-layer similarity coordinate, Eq. (5) |
| $\theta$ | = | nondimensional boundary-layer temperature, $T/T_s$ |
| $\lambda$ | = | mean free path of gas |
| $\mu$ | = | coefficient of viscosity |
| $\rho$ | = | density |
| $\omega$ | = | viscosity temperature dependence exponent ($\mu \sim T^\omega$) |

*Subscripts*

| | | |
|---|---|---|
| $e$ | = | conditions at boundary-layer edge |
| $g$ | = | conditions in gas |
| inv | = | inviscid flow |
| $s$ | = | stagnation value |
| $w$ | = | conditions on wall surface |
| $\infty$ | = | freestream conditions |

## Introduction

THE distribution of stagnation pressure $P_s$ is of great interest in design and computational fluid dynamics (CFD) validation studies of high-speed airbreathing engine inlets, hypervelocity test facility flows, and hypersonic vehicle flowfields.[1,2] Because the pitot tube probe is used to measure $P_s$, it is important to have an accurate basic theory to interpret the probe's readings in such applications. When the combination of flow conditions, speed, and probe nose size involve shock layer Reynolds numbers based on a diameter larger than 300, viscous effects are known[3,4] to have a negligible effect, and the classical Rayleigh supersonic pitot tube equation can be used to interpret the measurements. However, in hypersonic rarefied flows involving lower Reynolds numbers, the viscous and aerodynamic heating effects associated with the tube nose boundary layer become significant and introduce the need for corrections.

Numerical solutions[5] could, of course, serve this need; however, these are expensive to use for engineering studies and do not readily yield desirable physical insight and similitude laws. By focusing on the threshold of low Reynolds number effects associated with the continuum end of the rarefied flow regime, where a distinct shock wave still occurs on the probe nose, the present work offers an alternative analytical treatment that yields a closed-form relationship for the viscous correction to the Rayleigh equation. Anticipating that hypersonic applications may involve a cooled probe for survival,[1] our analysis includes the influence of an arbitrary probe surface temperature $T_w$ relative to the total temperature $T_s$ of the flow; an arbitrary type of gas is also allowed. We also examine, for the first time, the role of wall temperature and pressure slip, which turn out to be significant. It is felt that the present work yields an improved insight to observed pitot tube behavior at lower Reynolds numbers, especially as to the role of wall pressure slip and the wall temperature jump that drives it.

## Theoretical Formulation

The flowfield around the pressure port of a supersonic pitot tube is taken to be the stagnation region of a blunt-nosed two-dimensional or axisymmetric body (Fig. 1). This port is assumed to be very small (pin-hole) yet has a diameter much greater than the molecular mean free path near the surface. We note that the present emphasis is on

Presented as Paper 2004-2682 at the AIAA 37th Thermophysics Conference, Portland, OR, 28 June–1 July 2004; received 2 September 2004; revision received 8 February 2005; accepted for publication 9 February 2005. 

*Professor, Department of Aerospace Engineering. Associate Fellow AIAA.

**Table 1 Limiting hypersonic shock values for various gases**

| $\gamma$ | $\varepsilon_F$ |
|---|---|
| 5/3 | 1/4 |
| 7/5 | 1/6 |
| 9/7 | 1/8 |

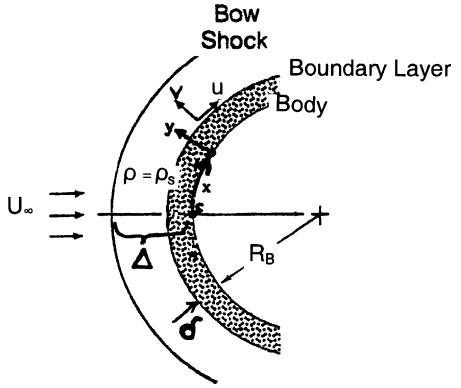


**Fig. 1 Schematic of two-layered model of hypersonic stagnation region shock layer.**

the role of the external flow events such as viscosity, heating, and pressure slip, rather than on the details of the probe geometry, hole size/length, etc. Such details do have some effect, but in the case of strongly hypersonic higher Reynolds number flows that we address, the available experimental data show them to play only a minor role.

Either monatomic or diatomic gases are considered that, in the shock layer, are in a fully excited rotational state and, in the diatomic case, in either a nonexcited or fully excited vibrational state. Table 1 shows the corresponding values of specific heat ratio and limiting hypersonic shock-layer density ratios. To bring out the essential viscous effects of interest in hypersonic flow, a two-layered model of the shock layer is employed: a thin outer region of constant-density adiabatic inviscid flow behind the shock, overlaying an inner viscous sublayer adjacent to the body surface. Chemically frozen flow without postshock dissociation is assumed throughout, and the flow within the inner viscous layer may be arbitrarily nonadiabatic.

**Purely Inviscid Analysis**

If one neglected viscosity and treated the entire shock layer as an inviscid flow with a constant density $\rho_s \cong \rho_\infty/\varepsilon_F$, where $\varepsilon_F \equiv (\gamma-1)/(\gamma+1)$ is the limiting hypersonic density ratio[6] across a normal shock in a gas of specific ratio $\gamma$ (Table 1), then stagnation pressure would have the postnormal shock value

$$P_{s,\text{inv}} \cong p_\infty + \rho_\infty U_\infty^2(1-\varepsilon_F) + (\varepsilon_F/2)\rho_\infty U_\infty^2 \tag{1}$$

where the last term is the constant-density contribution of the slight additional compression across the shock layer. For hypersonic flows where $\rho_\infty U_\infty^2 \gg p_\infty$, Eq. (1) may be further simplified on introduction of the freestream Mach number to the final working expression,

$$P_{s,\text{inv}}/p_\infty \cong (\gamma/2)M_\infty^2 \cdot [(\gamma+3)/(\gamma+1)] \tag{2}$$

Equation (2) is within 1% in accuracy of the hypersonic limit value of the Rayleigh formula[7]

$$P_{s,\text{Rayleigh}}/p_\infty = (\gamma/2)M_\infty^2 \cdot [(\gamma+1)^{\gamma+1}/4(\gamma)^\gamma]^{1/(\gamma-1)} \tag{3}$$

and is far simpler to use in view of the awkward multiple-exponent factor contained in Eq. (3). Also note that Eq. (1) implies a stagnation pressure coefficient of

$$Cp_{s,\text{inv}} \cong (\gamma+3)/(\gamma+1) = 1 + [2/(\gamma+1)] \tag{4}$$

which is slightly less than twice the classical incompressible value of unity because of nonisentropic shock wave compression.

**Inclusion of the Viscous Effect Within the Gas**

We now consider the presence of the inner viscous region by treating it as a boundary-layer type of flow in the vicinity of the stagnation line where the overlying inviscid flow has a density $\rho_s$ and a tangential velocity $U_{\text{inv}} \cong \beta_s x$ ($\beta_s$ being the inviscid stagnation point velocity gradient).[6] In this vicinity, it is known[6] that the compressible boundary layer possesses a self-similar behavior in terms of the stretched $y$ coordinate

$$\eta \equiv \sqrt{\frac{\beta_s(1+j)}{\rho_w\mu_w}}\int_0^y \rho\,\mathrm{d}y \tag{5}$$

By the introduction of the continuity-satisfying velocity variables $u = \beta_s x(\mathrm{d}f/\mathrm{d}\eta) \equiv \beta_s x f'(\eta)$ and $\rho^y = -\sqrt{(1+j)\rho_w\mu_w\beta_s}\,f(\eta)$, plus the nondimensional temperature $\theta(\eta) \equiv T/T_s = \theta_w + (1-\theta_w)\cdot g(\eta)$, and by invocation of the Chapman–Rubesin model $\rho\mu = \rho_w\mu_w$ with $\mu \sim T^\omega$ for the variable viscosity effect, the unknown functions $f$ and $g$ are found to be governed by the following $x$-momentum and energy equations, respectively:

$$f''' + ff'' = (1+j)^{-1}\left[(f')^2 - \theta_w + (1-\theta_w)g\right] \tag{6}$$

$$Prfg' + g'' = 0 \tag{7}$$

subject to the solid wall no-slip boundary conditions $f(0) = f'(0) = g(0) = 0$ and the outer inviscid flow matching conditions $f'(\infty) = g(\infty) = 1$, such that $f''(\infty)$ and $g'(\infty)$ vanish.

Equations (6) and (7) constitute the compressible Homann stagnation flow (see Ref. 8), within which our sought viscous stagnation pressure effect in the gas develops. This effect is of order $Re_s^{-1}$ in terms of the nose radius Reynolds number; hence, we have neglected the influence of the normal pressure gradient that contains the effect in formulating Eqs. (6) and (7) because this introduces only an error of order $Re_s^{-2}$ when these equations are used as an input to solving the normal momentum equation (see following text). Likewise, we can neglect the influence of wall slip on the solution to Eqs. (6) and (7) because this introduces an error of order $Re_s^{-3/2}$. Consequently, we may use the existing solutions of Eqs. (6) and (7) whose results have been extensively discussed and tabulated in detail.[9]

To obtain a first approximation for the boundary-layer effect on stagnation pressure correct to order $Re_s^{-1}$, we must integrate the normal pressure gradient across the layer as given by the basic $y$-momentum equation,[10]

$$\frac{1}{\rho}\frac{\partial p}{\partial y} = \frac{u^2}{R_B} - \left(u\frac{\partial v}{\partial x} + v\frac{\partial v}{\partial y}\right) + \frac{1}{\rho}\frac{\partial}{\partial x}\left(\mu\frac{\partial u}{\partial y}\right) + \frac{2}{3}\frac{1}{\rho}\left(2\mu\frac{\partial v}{\partial y} - \mu\frac{\partial v}{\partial x}\right) \tag{8}$$

wherein we have neglected the extremely small influence of streamwise diffusion, $\mu\partial^2 v/\partial x^2$. When the aforementioned similarity variable transformations are applied while care is taken to retain the compressibility effects on $\rho$ and $\mu$, Eq. (8) yields the following first-order differential equation governing $\mathrm{d}p/\mathrm{d}\eta$ in the gas along the stagnation line as $x \to 0$ (Fig. 1),

$$\frac{\rho_s(\mathrm{d}p/\mathrm{d}\eta)}{\beta_s\rho_w\mu_w} = \frac{\mathrm{d}}{\mathrm{d}\eta}\left\{\theta + \left[(1+j)\frac{f^2}{2} + \left(\frac{3+2j}{3}\right)f'\right]\right\} + (1-\theta_w)g'(0)\left[(1+j)\frac{f^2}{2} + f'\right]\exp\left(-Pr\int_0^\eta f\,\mathrm{d}\eta\right) \tag{9a}$$

where, in obtaining the last term in Eq. (9a), we have used the solution of Eq. (7) that

$$g'(\eta) = g'(0)\exp\left(-Pr\int_0^\eta f\,\mathrm{d}\eta\right) \tag{9b}$$

in terms of the known heat transfer property[9]

$$g'(0) \cong K_g Pr^{.4}(\rho_w\mu_w/\rho_s\mu_s)^{-.4} \tag{9c}$$

with $K_g = 0.570$ or 0.760 for two-dimensional or axisymmetric flow, respectively. Then, integrating Eq. (9a) from the surface $\eta = 0$, where $p = P_s$, to the outer boundary-layer edge, where $p = p_e \cong P_{s,\text{inv}} - \rho_s v_e(2/2)$, for the essentially constant-density flow at the boundary-layer edge $f = f_e$, and then using the aforementioned value of $\rho v$ evaluated at $f_e$, we ultimately obtain, after some arrangement, the following analytical relationship for the viscous correction to the inviscid stagnation pressure:

$$\frac{P_s - P_{s,\text{inv}}}{\rho_\infty U_\infty^2} = \frac{(\rho_w \mu_w / \rho_s \mu_s)(\beta_s R_B / U_\infty)}{Re_s} \times \{1 + (1 - \theta_w) g'(0)[(1 + j) I_1 + I_2]\} \tag{10a}$$

where

$$I_1 \equiv \int_0^\infty \frac{f^2}{2} \exp\left(-Pr \int_0^\eta f \, d\eta\right) d\eta \tag{10b}$$

$$I_2 \equiv \int_0^\infty f' \exp\left(-Pr \int_0^\eta f \, d\eta\right) d\eta \tag{10c}$$

An extensive numerical study reveals that these integrals are virtually independent of both $\theta_w$ and $j$, taking the values indicated in Table 2 as a function of Prandtl number.

A few observations are appropriate at this point. First, Eq. (10a) predicts that the gas side viscous correction for $T_w \le T_s$ is positive and proportional to $Re_s^{-1}$: This is in good agreement with a recent purely numerical study[5] of subsonic pitot tube behavior at low Reynolds number carried out by Williams (Fig. 2). From this comparison, we infer that the present work should be applicable down to $Re_s$ values of order 10 as intended. Second, it is seen that the viscous effect involves the product of three factors: 1) the term $(\beta s R_B / U_\infty) Re_s^{-1}$ that represents the contribution of the adiabatic ($T_w = T_s$) aspect of the problem, 2) the term $\rho_w \mu_w / \rho_s \mu_w \cong (T_w / T_s)^{\omega - 1}$ that accounts for the variable-viscosity effect associated with a cooled surface, and 3) the second term in braces that contains an explicit, positive contribution of the heat transfer across the boundary layer. (Actually, factor 1 contains an implicit compressibility effect in that the value of the nondimensional stagnation point velocity gradient depends markedly on whether the flow is incompressible or hypersonic.) The typical influence of factors 2 and 3 is illustrated in Fig. 3, where it can be seen that they both appreciably enhance the magnitude of the viscous stress-produced pressure increase.

Taken overall, Eq. (10a) indicates that the boundary-layer compressibility and heat transfer effects associated with surface cooling, although significantly modifying the magnitude of the viscous correction, do not alter the qualitative behavior already known from low-speed studies. Such effects, thus, do not essentially alter the basic physics governing the viscous effect in the gas, namely, that in

**Table 2 Values of normal pressure gradient integrals in Eq. (10a)**

| $Pr$ | $I_1$ | $I_2$ |
|---|---|---|
| 0.70 | 0.96 | 1.35 |
| 1.00 | 0.55 | 1.11 |

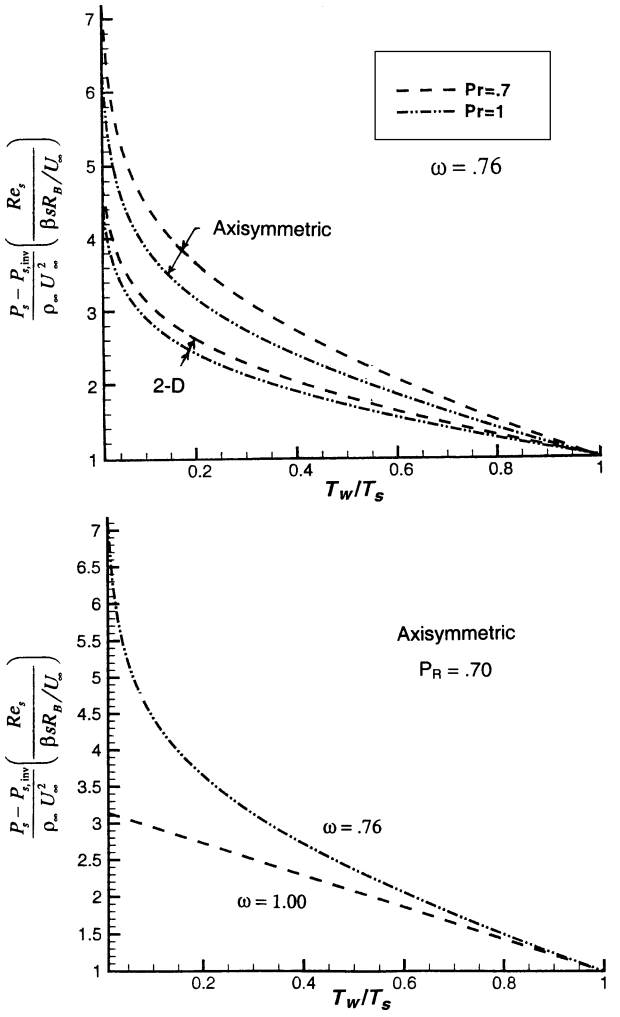


**Fig. 3 Nondimensional viscous effect on pitot pressure in gas vs wall temperature: effects of dimensionality, viscosity exponent, and Prandtl number.**

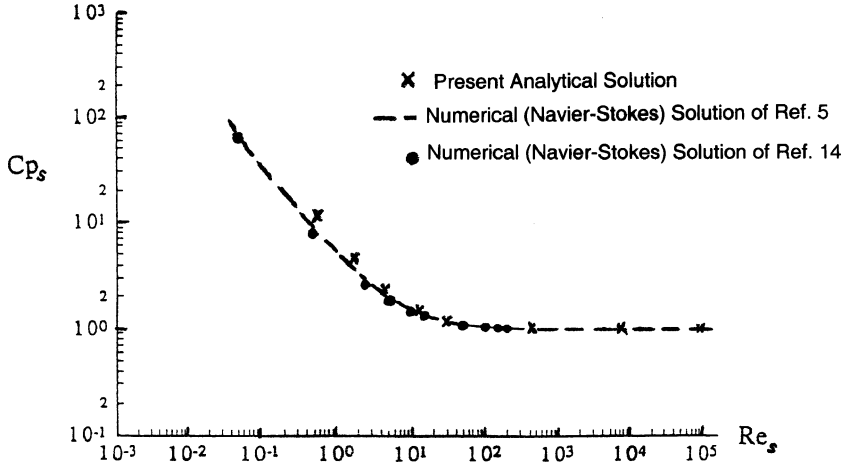


**Fig. 2 Axisymmetric pitot tube pressure coefficient vs shock layer Reynolds number in low-speed adiabatic flow.**

the immediate vicinity of the stagnation line the contribution of the tangential stress (which tends to decrease $P_s$) is about one-half of the contribution of the normal stress causing an increase in $P_s$ (Ref. 4). Viewed in this light, the predicted enhancing effects of cooling may be understood: In decreasing the boundary-layer thickness, it correspondingly enhances the net normal stress effect and, hence, the stagnation pressure.

We conclude this section by specializing the general result of Eq. (10) to the case of strongly hypersonic flow. For this purpose, we employ the shape-independent Newtonian theory value (widely used in hypersonic boundary-layer theory[6]) $\beta_s R_B/U_\infty = \sqrt{[2\varepsilon_F(1-\varepsilon_F)]}$. This expression brings out explicitly the important role of the shock-layer density ratio $\varepsilon_F$ (see following text). We note in connection with such a choice that the resulting neglect of a small nose shape effect has only a slight influence on our results compared with the additional effects of body dimensionality that are included in the theory. By the same token, although there is a small Reynolds number effect on $\beta_s$ in principle, this serves to correct results for the viscous/wall cooling/pressure slip effects on stagnation pressure that are already of higher order in $Re_D$ and so constitutes a higher-order influence that may be neglected in the present order of approximation.

Substituting the aforementioned Newtonian value, using $\rho_w\mu_w/\rho_s\mu_w \cong (T_w/T_s)^{\omega-1}$ plus Eq. (9c) and dividing through by the Newtonian pressure of Eq. (4), we, thus, obtain the following working form of our gas side viscous correction expressed as a fraction of $P_{s,\text{inv}}$:

$$\frac{P_{s,g}}{P_{s,\text{inv}}} \cong 1 + \frac{2\Gamma_G(T_{wg}/T_s)^{\omega-1}}{\left(Re_s/\sqrt{\varepsilon_F}\right)} \times \left\{1 + Pr^{.4}K_g\left(\frac{T_{w_g}}{T_s}\right)\left(1-\frac{T_{w_g}}{T_s}\right)(1+j)I_1 + I_2\right\} \qquad (11)$$

where $\Gamma_G \equiv \sqrt{[2(1-\varepsilon_F)]}(\gamma+1)/(\gamma+3)$. Although $\Gamma_G$ appears to depend on the gas, in fact, it turns out to be virtually a constant $\cong\sqrt{2}/2$ over the entire range of specific heat ratio values of practical interest (Table 3) Consequently, it is seen from Eq. (11) that the modified Reynolds number parameter $Re_{s\varepsilon} \equiv Re_s/\sqrt{\varepsilon_F}$ completely absorbs the effect of gas type (neglecting a negligible $Pr^{.4}$ effect) for the gases of aerodynamic interest. This is clear in Fig. 4, where $(P_{s,g}-P_{s,\text{inv}})/P_{s,\text{inv}}$ from Eq. (11) vs $Re_{s_\varepsilon}$, is seen to depend only on $T_w/T_s$ over a wide range of $\varepsilon_F$ values. The foregoing is an important result of the present theory because it lends basic support to the well-documented empirical fact that the correlation of experimental data on hypersonic pitot tubes in terms of $Re_{s_\varepsilon}$ completely accounts for all types of gases.[11] Conversely, these correlations lend experimental support to our theory.

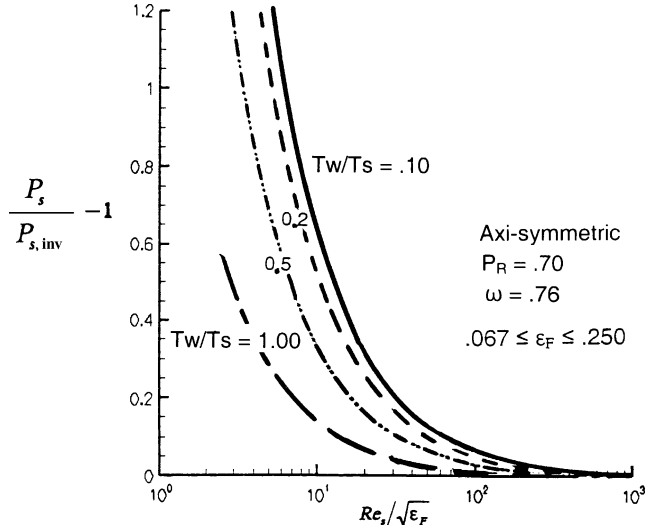


**Fig. 4 Correlation of gas-type effect by modified Reynolds number parameter $Re_s/\varepsilon_F^{1/2}$.**

**Table 3 Tabulation of parameter $\Gamma_G$ in Eq. (11) vs $\gamma$**

| $\gamma$ | $\Gamma_G$ |
|---|---|
| 1.10 | 0.710 |
| 1.25 | 0.707 |
| 1.40 | 0.705 |
| 1.55 | 0.700 |
| 1.70 | 0.695 |
| 1.85 | 0.690 |

As will be shown hereafter, Eq. (11) for adiabatic hypersonic flow is in good agreement with experiment for uncooled pitot tubes. However, when heat transfer is present, Eq. (11) must be corrected for the phenomenon of pressure slip at the wall, which alters the actual pressure sensed in the solid wall surface.

**Intervention of Wall Pressure Slip**

Equation (11) pertaining to the gas is unaffected by slip phenomena to order $Re_s^{-1}$, as we have noted. However, at lower Reynolds numbers in the presence of cooling, the slip effect on pressure (which is usually ignored in discussions of slip) can, in fact, cause a significant negative pressure jump from the gas to the wall surface that intervenes to a lower order in $Re_s$, namely, to order $Re_s^{-1/2}$. Consequently, we examine the role of pressure slip in detail for a hypersonic body stagnation region.

It is usually not mentioned in the hypersonic flow literature that the well-known temperature slip phenomena, given to first order by

$$T_{g_w} \cong T_w - \frac{75\pi}{128}\left(\frac{2-\alpha}{\alpha}\right)\lambda w\left(\frac{\partial T}{\partial y}\right)_{g,w} \qquad (12)$$

is, in fact, accompanied by the heat transfer-driven pressure slip[12]

$$\frac{p_{w,g}}{p_w} \cong 1 + \frac{15}{16}\frac{(2-\alpha)}{(\alpha)}\frac{\lambda w}{T_{g_w}}\left(\frac{\partial T}{\partial y}\right)_{w,g} \qquad (13)$$

where $p_w$ is the actual pressure sensed on the wall. Equation (12a) is clearly of relevance to the present problem. To assess this further, we specialize Eqs. (12a) and (12b) to the case of strongly hypersonic stagnation region flow by introducing the standard[13] expression $\lambda \cong \mu\sqrt{(\pi RT/2)}/p$ plus the stagnation values of wall temperature gradient [Eq. (9c)], velocity gradient, and inviscid stagnation pressure; the result is

$$T_w \cong T_{wg} + K_{w_t}\frac{(T_w/T_s)^{\omega/2}}{Re_{s_\varepsilon}^{\frac{1}{2}}}(T_s - T_w) \qquad (14)$$

$$\frac{p_{w,g}}{p_w} \cong 1 + Kw_p\frac{(T_w/T_s)^{\omega/2}}{T_w/T_s}\frac{(1-T_w/T_s)}{\left[Re_{s_\varepsilon}\right]^{\frac{1}{2}}} \qquad (15)$$

where $K_{w_t} \equiv 2.74K_G Pr^{.4}(2-\alpha)/\alpha$ and $K_{w_p} \equiv 1.40K_G Pr^{.4}(2-\alpha)/\alpha$. These stagnation relations reveal several important features about nonadiabatic wall temperature and pressure slip. First, we note that they also depend on the modified Reynolds number parameter $Re_s/\sqrt{\varepsilon_F}$ as seen earlier in the gas-phase analysis. Second, the Reynolds number dependence scales as $Re_{s_\varepsilon}^{-1/2}$ instead of $Re_s^{-1}$, so that the pressure slip effect will intervene at higher Reynolds numbers than those where the gas-side viscous effect [Eq. (11)] becomes significant and ultimately dominates. Third, in contrast to what is usually asserted about slip effects in the literature, the pressure slip effect actually increases with cooling because it is inversely proportional to $T_w$.

If we now introduce Eq. (11) for the gas-side pressure into Eq. (15) and then solve for the wall surface pressure sensed by the pitot tube orifice, we obtain the following working relationship up to and

including terms of order $Re_{s_\varepsilon}^{-1}$:

$$\frac{P_w}{P_{s,\text{inv}}} = 1 - C_s \frac{(1 - T_w/T_s)}{Re_{s_\varepsilon}^{\frac{1}{2}}} + \frac{C_G + C_s^2(1 - T_w/T_s)^2}{Re_{s_\varepsilon}} \tag{16a}$$

$$C_G \equiv \sqrt{2}\left(\frac{T_w}{T_s}\right)^{\omega - 1}\left\{1 + \left(1 - \frac{T_w}{T_s}\right)Pr^4 K_G[(1+\varepsilon)I_1 + I_2]\left(\frac{T_w}{T_s}\right)^{.4(1-\omega)}\right\} \tag{16b}$$

$$C_s \equiv 1.395 K_G Pr\left(\frac{2-\alpha}{\alpha}\right)\left(\frac{T_w}{T_s}\right)^{\omega/2 - 1} \tag{16c}$$

Examination of Eq. (16) indicates that the wall pressure slip effect causes the stagnation pressure to first decrease with decreasing $Re_{s_\varepsilon}$ before the gas-phase pressure rise effect subsequently takes over and dominates at even lower Reynolds numbers. Experimental data on cooled hypersonic pitot tubes support this prediction as discussed later.

## Comparisons with Experiment

### Adiabatic Surfaces

In the absence of heat transfer and, hence, of the aforementioned wall slip effects, the present theory predicts that the normal stress effect within the boundary layer causes a monotone increase in stagnation pressure with decreasing Reynolds number proportional to $Re_{s_\varepsilon}^{-1}$. This is in both qualitative and quantitative agreement with several experimental studies in the near-continuum regime. First, as shown in Fig. 2, the low-speed version of the present theory [obtained by setting $\varepsilon_F = 1$, $\rho_w \mu_w = \rho_s \mu_s$ and using the incompressible value of $\beta_s$ in Eq. (10)] when plotted vs $Re_s$ agrees very well with the results of several full Navier–Stokes numerical solutions[5,14] for spherically nosed probes. Second, in the case of pitot tube studies in hypersonic flow, the predictions from the adiabatic version of Eq. (11) are in good agreement with typical pressure vs $Re_D$ data[15] obtained for uncooled hemispheric probes (Fig. 5). (In Ref. 15, no discernable probe orifice size effect for orifice diameters less than 0.2 probe diameter is cited.) Clearly, the present theory, for adiabatic flows at least, gives a valid description of the 10–20% viscous effect down to $Re_s \geq 10$ as intended. Third, on a qualitative basis, the present predictions are in accord with several earlier numerical studies of hypersonic fully viscous shock layer flow.[16,17]

### Nonadiabatic Surfaces

Figure 6 is a typical selection of results from a comprehensive 1966 Arnold Engineering Development Center (AEDC) experimental study[11] of highly cooled hemispheric and flat-nosed pitot tubes in hypersonic flow where nondimensional stagnation pressures are correlated in terms of the modified Reynolds number $Re_{s_\varepsilon} \equiv Re_D/\sqrt{\varepsilon_F}$ identified in the present work. These data span the full near-continuum regime $10 \leq Re_D \leq 10^3$ of interest here and were observed to be small orifice size independent. Notwithstanding a modest probe shape effect discernable in Fig. 6, the overall trend of the data with decreasing $Re_\varepsilon$ regardless of shape is in clear agreement with the foregoing theoretical observations regarding the intervening effect of wall pressure slip in reducing the pressure at intermediately low Reynolds numbers. This view is further

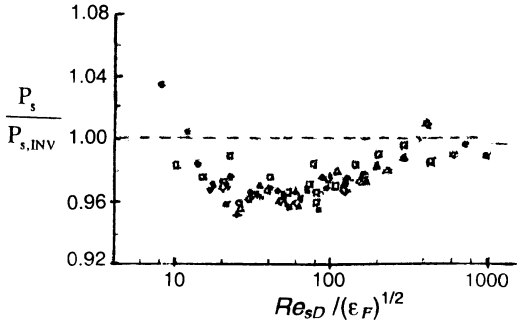


**a) Flat-nosed probes in Ar with $T_w = 0.1$–$0.3\ T_s$**

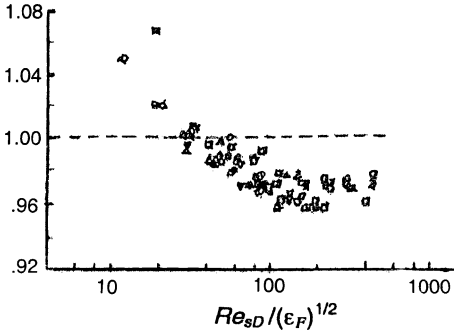


**b) Hemispherically nosed probes in Ar with $T_w = 0.1$–$0.2\ T_s$**

**Fig. 6 Experimental data from AEDC study[11] of highly cooled pitot tubes in hypersonic flow.**

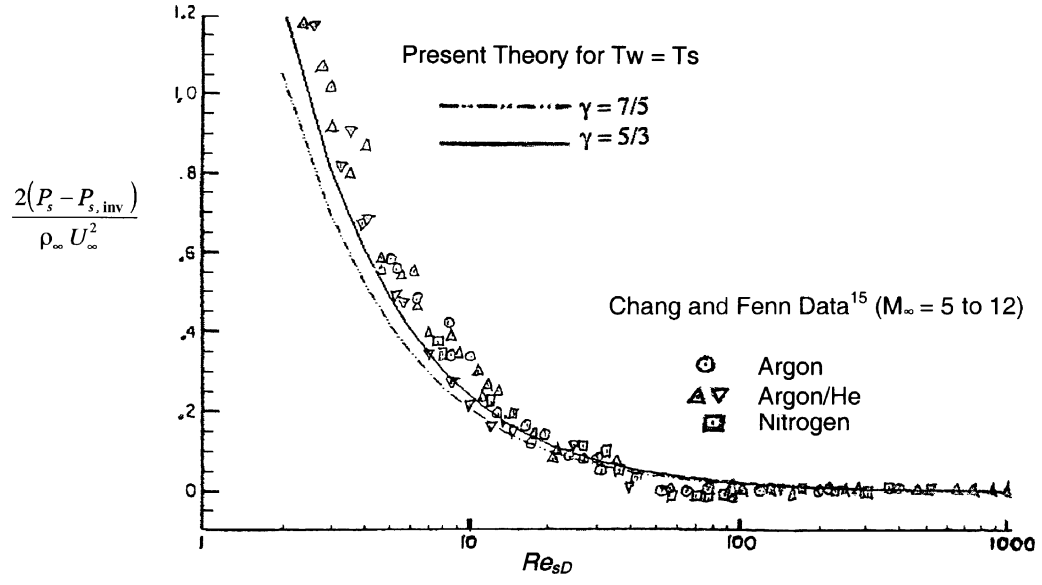


**Fig. 5 Comparison of present theory with experimental pitot data on uncooled hemispherical probes in hypersonic flow.**

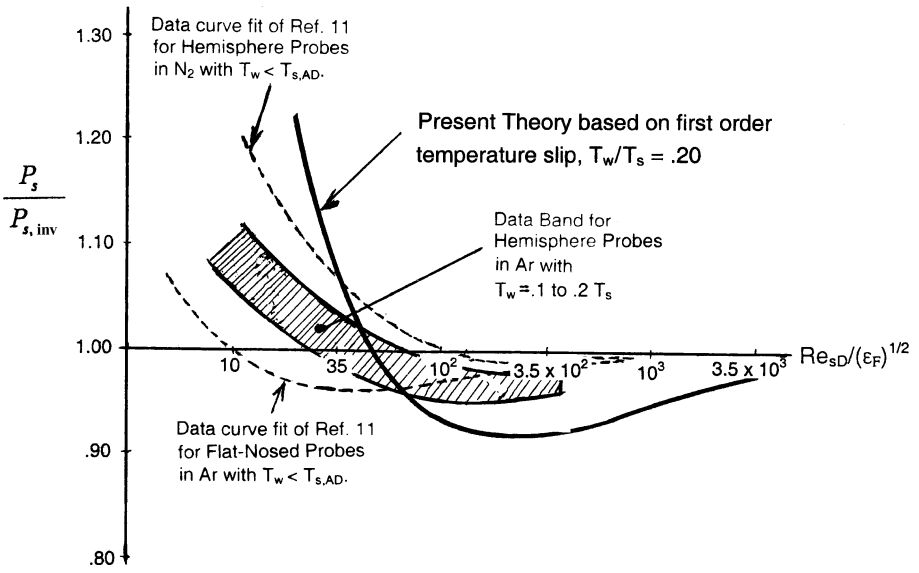


**Fig. 7 Comparison of present theory including wall pressure slip effect with experimental data.[11]**

reinforced by a detailed comparison of some sample data with the predictions of Eq. (16), as shown in Fig. 7. When the data scatter is allowed for, it is seen that the theory is in reasonably good agreement as to the rapidly reversing behavior of pressure vs decreasing Reynolds number down to around $Re_{s_\varepsilon} \geq 10$, as well as to the value of $Re_{s_\varepsilon}$ in correlating the data.

## Summary

The present study has revealed that near-continuum low Reynolds number effects on hypersonic stagnation pressure derive from two opposing physical events: 1) the normal stress within the boundary layer that causes pressure to increase slightly with decreasing Reynolds number as $Re_D^{-1}$ and 2) a significant wall pressure slip that only occurs with cooling and that causes a decrease in stagnation pressure with decreasing $Re_D$ as $Re_D^{-1/2}$, thus, dominating at intermediately low $Re_D$. Moreover, it was found that the influence of gas type is completely absorbed by using the modified Reynolds number parameter $Re_D/\sqrt{\varepsilon_F}$. The derived relationships governing these findings appear generally supported by available experimental data.

It is felt that the present work provides an improved insight to observed pitot tube behavior at lower Reynolds numbers. In particular, our conclusions strongly suggest that wall pressure slip (and, hence, the wall temperature slip driving it) should be taken into account in purely numerical (CFD) studies of the problem if physically realistic results are to be obtained in the presence of surface cooling; indeed, contrary to general belief, this slip effect on pressure is more, not less, significant for highly cooled surfaces. In this regard, numerical studies including the complete probe geometry using the discrete simulation Monte Carlo method would be a valuable complement to the present work because recent versions of the method now appear applicable to near-continuum flow conditions.

## Acknowledgments

The provision of several key documents containing experimental data and references thereto by Frank Lu of the University of Texas at Arlington is gratefully acknowledged. Appreciation is also extended to Patrick Trizila, an Iowa State University student, for assistance in figure preparation.

## References

[1]Magin, T., and Degrez, G., "Cooled Pitot Probe in Inductive Air Plasma Jet: What Do We Measure?," 2nd International Symposium on Atmospheric Reentry Vehicles, Paper No. 3, Paris, March 2001.

[2]Emanuel, G., "The Role of Stagnation Pressure for Air-Breathing Hypersonic Propulsion," AIAA Paper 2003-928, Dec. 2003.

[3]Issa, R. I., "Rise of Total Pressure in Frictional Flow," *AIAA Journal*, Vol. 33, No. 4, 1995, pp. 772–774.

[4]Van Ondhensden, B. W., "Comment on 'Rise of Total Pressure in Frictional Flow,'" *AIAA Journal*, Vol. 35, No. 2, 1996, pp. 426, 427.

[5]Williams, J. C., "Rise of Total Pressure Near the Stagnation Point on a Sphere," *AIAA Journal*, Vol. 40, No. 3, 2002, pp. 576–580.

[6]Hayes, W. D., and Probstein, R. F., *Hypersonic Flow Theory*, Academic Press, New York, 1959, pp. 150–162.

[7]Anderson, J. D., *Fundamentals of Aerodynamics*, 3rd ed., McGraw–Hill, New York, 2001, p. 497.

[8]Schlichting, H., *Boundary Layer Theory*, 7th ed. McGraw–Hill, New York, 1979, pp. 95–101.

[9]White, F. M., *Viscous Fluid Flow*, 2nd ed., McGraw–Hill, New York, 1991, pp. 246–248.

[10]Kuethe, A. M., and Chow, Y. C., *Foundations of Aerodynamics*, 5th ed., Wiley, New York, 1998, pp. 519–521.

[11]Potter, J. L., and Bailey, A. B., "Pressures in Stagnation Regions of Blunt Bodies in Rarefied Flow," *AIAA Journal*, Vol. 2, No. 4, 1964, pp. 743–745.

[12]Gupta, R. N., "Two- and Three-Dimensional Analysis of Hypersonic Nonequilibrium Low-Density Flows," *Journal of Thermophysics and Heat Transfer*, Vol. 10, No. 2, 1996, pp. 267–276.

[13]Vincenti, W. G., and Kruger, C. H., *Introduction to Physical Gas Dynamics*, Wiley, New York, 1965, p. 47.

[14]LeClair, B. P., Hamielec, A. E., and Pruppacher, H. R., "A Numerical Study of the Drag on a Sphere at Low and Intermediate Reynolds Numbers," *Journal of the Atmospheric Sciences*, Vol. 27, No. 2, 1970, pp. 308–315.

[15]Chang, J. H., and Fenn, J. B., "Viscous Effects on Impact Pressure Measurements in Low Density Flows at High Mach Numbers," *Rarefied Gas Dynamics*, Vol. 1, 1969, pp. 835–838.

[16]Kao, M. C., "Hypersonic Viscous Flow Near the Stagnation Streamline of a Blunt Body: II. Third-Order Boundary-Layer Theory and Comparison with Other Methods," *AIAA Journal*, Vol. 2, No. 11, 1964, pp. 1989–1906.

[17]Probstein, R. F., and Kemp, N., "Viscous Aerodynamic Characteristics in Hypersonic Rarefied Gas Flow," *Journal of the Aerospace Sciences*, Vol. 27, March 1960, pp. 174–192.